JOC The Journal of Organic Chemistry

Article

Synthesis of Solution-Processable Donor-Acceptor Pyranone dyads for White Organic Light Emitting Devices

CHANDRA PRAKASH SHARMA, Neeraj M. Gupta, Jagriti Singh, Rohit Ashok Kumar Yadav, Deepak Kumar Dubey, Kundan Singh Rawat, Ajay Kumar Jha, Jwo-Huei Jou, and Atul Goel

J. Org. Chem., **Just Accepted Manuscript** • Publication Date (Web): 22 May 2019

Just Accepted

is published by the American Chemical Society. 1155 Sixteenth Street N.W., Washington, DC 20036

Synthesis of Solution-Processable Donor-Acceptor Pyranone dyads for White Organic Light Emitting Devices

Chandra P. Sharma,[†#] Neeraj M. Gupta,[†#] Jagriti Singh,[†#] Rohit Ashok Kumar Yadav,[§] Deepak Kumar Dubey,[§] Kundan S. Rawat,[†] [‡]Ajay K. Jha,[†] Jwo-Huei Jou[§] and Atul Goel*[†,‡]

[†]*Fluorescent Chemistry Lab, Medicinal and Process Chemistry Division, CSIR-Central Drug Research Institute, Lucknow 226031, India*

[§]*Department of Materials Science and Engineering, National Tsing Hua University, Hsinchu, Taiwan 30013, Republic of China*

[‡]*Academy of Scientific and Innovative Research, Ghaziabad 201 002, India*

E-mail: atul_goel@cdri.res.in

ABSTRACT

A series of donor-acceptor pyranones (**3a-m, 4a-h)** was synthesized using α-oxo-ketene-*S*,*S*-acetal as synthon for their application as emissive materials for energy-saving organic light emitting devices (OLEDs). Among them, five pyranones **3f**, **3g**, **3h, 3m,** and **4e** exhibited highly bright fluorescence in the solid state and weak or no emission in the solution state. Photophysical analysis of these dyes revealed that only **3f** and **3m** showed aggregation-induced emission behaviour in THF/water mixture (0-99%) with varying water fractions (f_w) leading to bright fluorescence covering entire visible region, while other derivatives **3g**, **3h** and **4e** did not show any fluorescence signal. The computational studies of the compounds revealed that the longer wavelength absorption originates from HOMO to LUMO electronic excitation. These dyes exhibited good thermal stability with 5% weight loss temperature in the range of 218-347 ^{o}C. The potential application of the donor-acceptor pyranone dyads was demonstrated by fabrication of solution-processed OLEDs. Remarkably, OLED devices prepared using highly emissive compounds 6-(anthracen-9-yl)-4-(methylthio)-2-oxo-2*H*-pyran-3-carbonitrile (**3m**) and 6-(4-methoxyphenyl)-4-(methylthio)-2-oxo-

2*H*-pyran-3-carbonitrile (**3f**) displayed pure white emission with CIE coordinates of (0.29, 0.31) and (0.32, 0.32), respectively. Additionally, the resultant devices exhibited external quantum efficiency (EQE) of 1.9% and 1.2% at 100 cd m^{-2}, respectively.

INTRODUCTION

Solid-state white organic light emitting devices (WOLEDs) have attracted a great deal of attention owing to their potential use in day-to-day lighting systems with long lifetime, high brightness and low energy consumption.[1-3] These energy-saving devices are now on the verge of becoming an alternative source of light to conventional incandescent and fluorescent lamps.[4]

Typically, WOLEDs can be fabricated by the mixing or stacking of three primary colors (red, green, and blue)[5-7] emitting materials or two complementary colors (yellow and blue)[8] emitters into a single or multiple emissive layer either via dry or solution process. However, these multi-layered or multi-dopant device structures not only results in increased fabrication difficulty and costs, but also yield numerous operational problems making them a less attractive approach for generating white light emitting devices. Moreover, these multi-component based systems are associated with many other challenges such as improper phase segregation, low color rendering index, poor efficiency and most importantly less reproducibility.[9-12]

Over the last few years, numerous approaches have been developed for fabrication of WOLEDs and it has become a front-line research field of academia as well as industries (Table S1 in Supporting Information). WOLEDs have been fabricated by employing inorganic substances,[10-11] inorganic-organic hybrid systems,[12] polymers,[13-15] quantum dots,[16-17] rare-earth elements,[18-19] and archetypal organic phosphors.[20] Among them, single component based white light organic emitters have captured remarkable attention due to their ability to be transformed in a film, good thermal and electrochemical stability, excellent color tunability and high efficiency as well as simple fabrication process.[21-24] To achieve efficient white light emission, several mechanisms/concepts have been

demonstrated that include inter-/intra-molecular charge transfer (ICT),[25-27] Excited-state intramolecular proton transfer (ESIPT),[28,29] Frustrated Energy Transfer,[30] excimers,[31,32] or aggregation-induced emission (AIE).[33,34]

It has been well-documented that donor-acceptor based organic molecular frameworks are potential compounds for preparing light emitting devices with high quantum efficiency, chemical and thermal robustness, color tunability.[35] By screening a small library of donor-acceptor based pyranones and π-conjugated systems, we recently discovered first solution-solid dual emissive AIE luminogen dihydropyrano-indolizine **DPI-7**, and developed multi-color bright light emitting solid compounds by modulating donor-acceptor and chromophoric moieties.[36] We observed that few pyranone derivatives in the library showed bright fluorescence in the solid state and envisaged that they may be tuned for preparing multicolour/white optoelectronic devices by modulating donor-acceptor and chromophoric moieties. To our surprise, no systematic investigations have been made earlier for exploring the optoelectronic properties of pyranone derivatives. Aiming to search for new white-emissive fluorophores and to enhance our understanding with pyranones having push-pull characteristics, herein, we report synthesis, photophysical, electrochemical, thermal, and electroluminescent properties of a series of pyranones with different donor-acceptor functionalities for developing organic electronic devices.

RESULTS AND DISCUSSION

Synthesis of Fluorescent Compounds

For the last two decades, our research group has been involved in developing new fluorescent aromatic compounds using the chemistry of 2-pyranones. We have demonstrated how swapping of the electron donor and acceptor groups onto an aromatic scaffold modulate the optical properties of fluorenes.[37] Recently we have reported pyranones and their derived fluoranthenes, pyrenylarenes

and non-planar benzo[*f*]quinolines/acridines as efficient light emitting materials for OLED applications.[36,38] Therefore, in order to tune the photophysical properties of pyranones for their potential use in optoelectronic devices, it was imperative to prepare pyranones having different donor-acceptor and chromophoric moieties. There are many synthetic approaches reported in the literature for the synthesis of 2-pyranones.[39-41] We found Tominaga *et al.* protocol[41a] suitable for the synthesis of various donor-acceptor based 2-pyranone derivatives. The reaction of α-oxo-ketene-*S*,*S*-acetal **1** with different aryl ketones **2a-m** in the presence of potassium hydroxide in dimethylsulfoxide at room temperature afforded 6-aryl-4-methylthio-2*H*-pyran-3-carbonitriles **(3a-m)** in good yields. Further methylthio group was replaced with different secondary amine in methanol to afford 4-amino-6-aryl-2-oxo-2*H*-pyran-3-carbonitriles **(4a-h)** in good yields (Scheme 1).

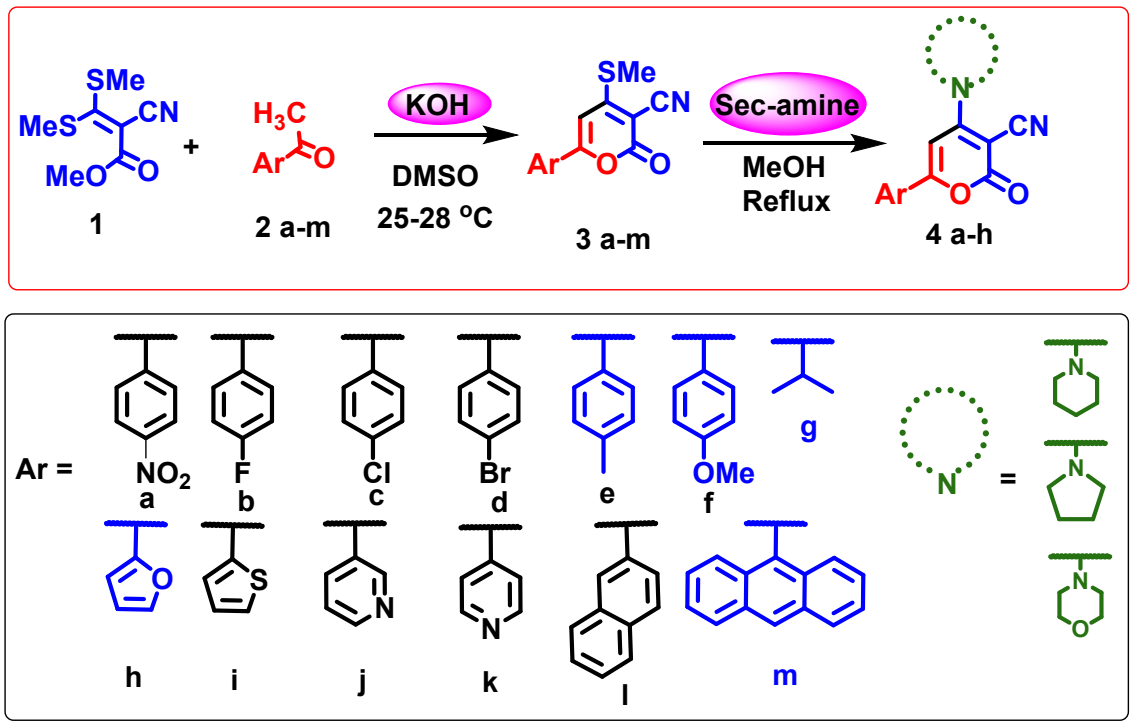

Scheme 1. Synthesis of pyranone derivatives.

Photophysical Properties

The photophysical properties of the synthesized compounds **3a-m** and **4a-h** were examined by their UV-vis absorption and photoluminescence (PL) spectra both in solution as well as in the solid state. All the synthesized compounds **3a-m** and **4a-h** were found to be non-fluorescent (NF) or weak fluorescent in DMSO solution. Interestingly, some of the pyranones having electron rich moiety at position 6 showed good to excellent fluorescence in solid state. The bright fluorescence of these molecules in solid state may be due to restriction of molecular motion with effective charge transfer in the solid state leading to radiative decay. On the contrary, compound having electron withdrawing group (4-nitrophenyl) at position 6 of pyranone exhibited no solid state fluorescence due to ineffective charge transfer (Table 1). Among them, compounds **3f, 3g, 3h, 3m,** and **4e** showing highly bright fluorescence (intensity > 750 au at slit width of 2.5 nm) in the solid state were selected for further studies.

Table 1. Photophysical properties of pyranones **3a-m** and **4a-h**.

Sr. No.	Ar	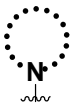	$\lambda_{max, abs}$[a] (nm)	$\lambda_{max, em}$[b] (nm)	Intensity[c] (au)
3a	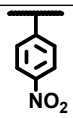	--	398	NF	NF
3b		--	405	505	600
3c		--	410	511	271
3d		--	414	485	75
3e		--	410	491	546

3f		--	394, 340	485	>1000[d]
3g		--	347, 296	424	>1000[d]
3h		--	396, 344	500	937[d]
3i		--	428	528	8
3j		--	400	449	43
3k		--	408	458	63
3l	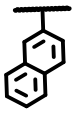	--	395	504	271
3m	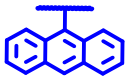	--	400, 357, 296	572	776[d]
4a			320	450	310
4b			315	458	656
4c			325	488	506
4d			315	451	384
4e			323	466	>1000[d]
4f			321	451	332
4g			405	512	387

4h	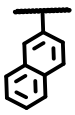		327	481	425

[a]Longest wavelength absorption maximum in DMSO; [b]Solid state fluorescence emission maximum in powder, [c]Solid state PL intensity at slit width 2.5 nm. [d]Quantum Yield: **3f**: 6.88%; **3g**: 4.36%; **3h**: 4.20%; **3m**: 5.10%; **4e**: 10.57%.

UV-vis and PL spectra of selected compounds **(3f, 3g, 3h, 3m, and 4e)** are given in Figure 1. The PL maxima of substituted pyranones **(3f, 3g, 3h, 3m, and 4e)** in solid state (powder) showed blue to orange fluorescence (λ_{max} 424-572 nm). Due to the presence of planar π-conjugated anthracene moiety at position 6 of substituted pyranone **3m**, it showed strong red shift with emission maximum at 572 nm as compared to other derivatives **(3f, 3g, 3h,** and **4e)**, while in the absence of aromatic ring at the 6-position of pyranones like in **3g,** it showed a blue shift with emission maximum at 424 nm.

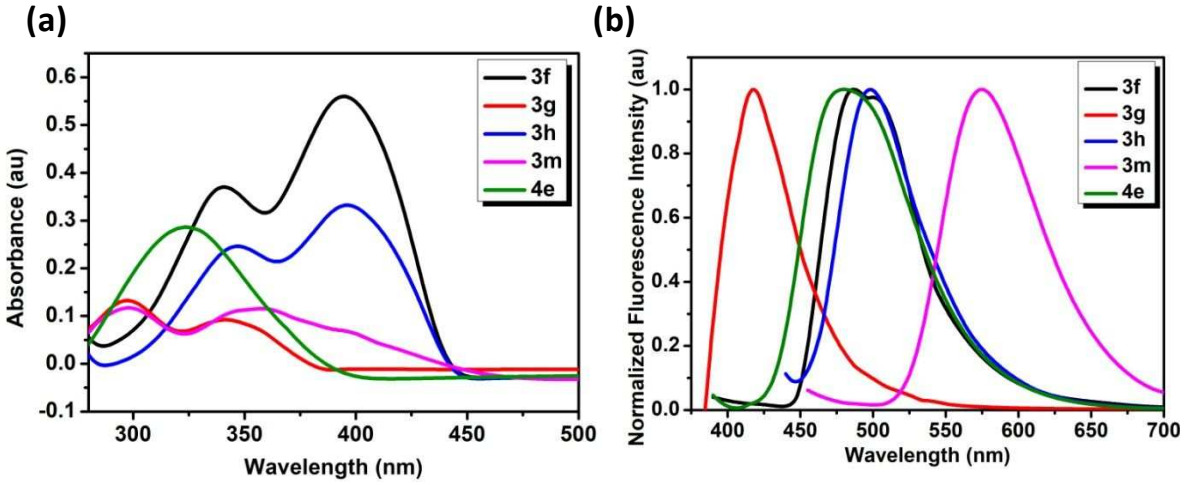

Figure 1. (a)Absorption (in DMSO) and (b) solid state emission spectra of **3f, 3g, 3h, 3m,** and **4e** in powder form

***Aggregation Induced Emission Property*:** In order to understand the mechanism of bright fluorescence of these dyes in the solid state and weak or no emission in the solution state, we investigated the aggregation-induced emission (AIE) property of the compounds **3f**, **3g, 3h, 3m,** and **4e**. For this purpose, the fluorescence study was conducted in THF/water mixture (0-99%) with

varying water fractions (f_w). It was observed that only **3f** and **3m** showed aggregation-induced emission behaviour, while other derivatives **3g**, **3h** and **4e** did not show any fluorescence signal. Further we found that upon increasing the water fraction (f_w) in THF solution of **3f**, the fluorescence intensity increased gradually from 60% to 90% with emission maximum at 470 nm. Surprisingly, at 99% water fraction, the emission of the dye **3f** became broad and shifted from blue to green region with maximum at 520 nm (Figure 2a). Similarly, upon increasing the water fraction (f_w) in THF solution of **3m**, the fluorescence intensity increased gradually from 0% to 90% with emission maximum at 530 nm and at 99% water fraction, the emission became broad and bathochromically shifted from green to yellow region with maximum at 542 nm (Figure 2b). Interestingly, when the f_w reached 99%, a drastic enhancement was observed in the emission intensity (upto 26-fold in **3f** and 15-fold in **3m**) as compared to the pure THF solution. These results implicated that both **3f** and **3m** showed aggregation induced emission property with broad spectra covering entire visible region and they may be promising candidates for WOLEDs.

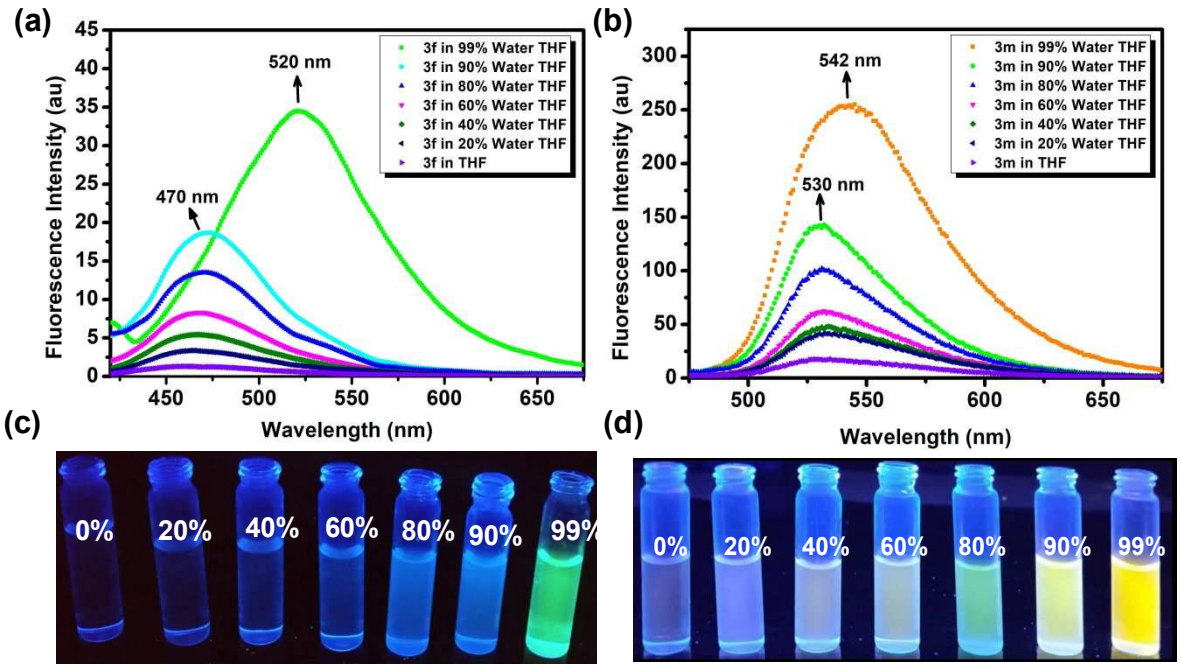

Figure 2. Fluorescence spectra of (a) pyranone **3f** and (b) **3m** with increasing water fraction [from 0 to 99% (v/v) water in THF]. Images of (c) **3f** and (d) **3m** in THF with varying water fraction taken under UV light illumination (λ_{ex} = 365 nm).

Fluorescence life time decay analysis:

Furthermore, Time-correlated single photon counting (TCSPC) analysis was performed to measure the average fluorescence lifetime of the aggregates of **3f** and **3m** in 99% water in THF taking Ludox as a prompt (Figure 3). The fluorescence life time decay profile of **3f** and **3m** in 99% water in THF nicely fitted with tri-exponential function as shown in Figure 3. The average fluorescence lifetime of aggregates **3f** and **3m** was found to be 2.6 ns and 3.0 ns respectively.

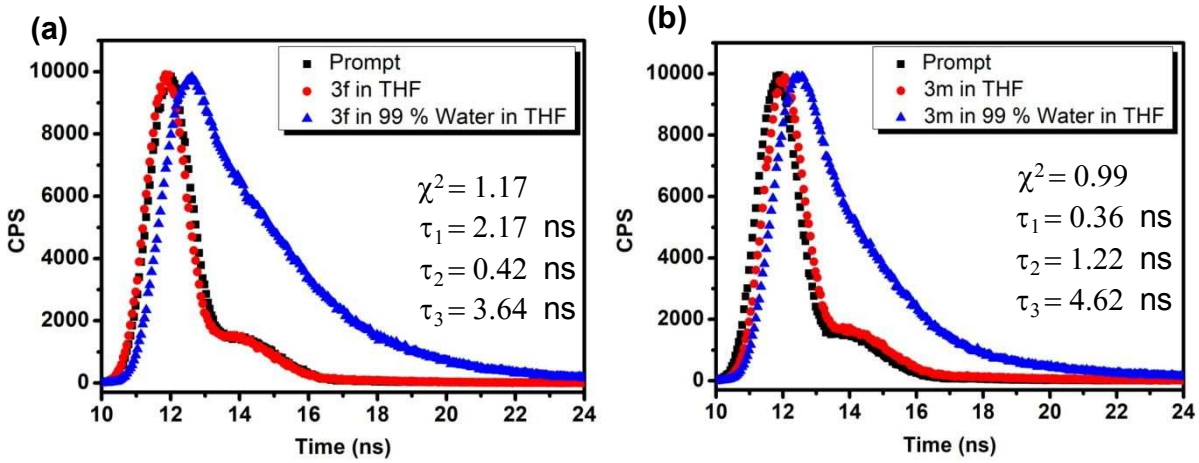

Figure 3. Time-resolved fluorescence decay plot of (a) dye **3f** and (b) dye **3m** in pure THF and 99% water in THF solution at 25 °C using a nano-LED of 390 nm as the light source.

Computational Studies

To examine the electronic properties of the compounds **3f**, **3g, 3h, 3m** and **4e,** time-dependent density functional theory (TDDFT) calculations were performed with a Gaussian 09 package.[42] The geometries were optimized at DFT/B3LYP level using a 6-31G (d, p) basis set. TDDFT calculations were performed using a B3LYP/6-31++G (d, p) method.

Figure 4 showed the theoretically computed molecular orbitals in the ground states for the representative compounds **3f, 3g, 3h, 3m,** and **4e**. TDDFT calculations indicated that the charge density distribution of HOMO for compound **3f** was spread over the phenyl, pyran and partially at sulphur atom and in LUMO the charge density was mainly shifted towards the pyran and –SMe segment. For compound **3g,** the charge distribution in HOMO was majorly localised on the pyran unit and –SMe group and in LUMO it was localised at sulphur atom of –SMe group, pyran ring and –CN group. For compound **3h** the charge density in HOMO was localised on the furan and pyran unit and in LUMO it was localised mainly on the pyran core, sulphur atom and partially on furan unit. For compound **3m** the charge density in HOMO was localised on the anthracene unit and in LUMO it was localised on anthracene and pyran moiety having nitrile and -SMe group. For compound **4e** the charge densities in HOMO and LUMO were localised on the phenyl and pyran rings.

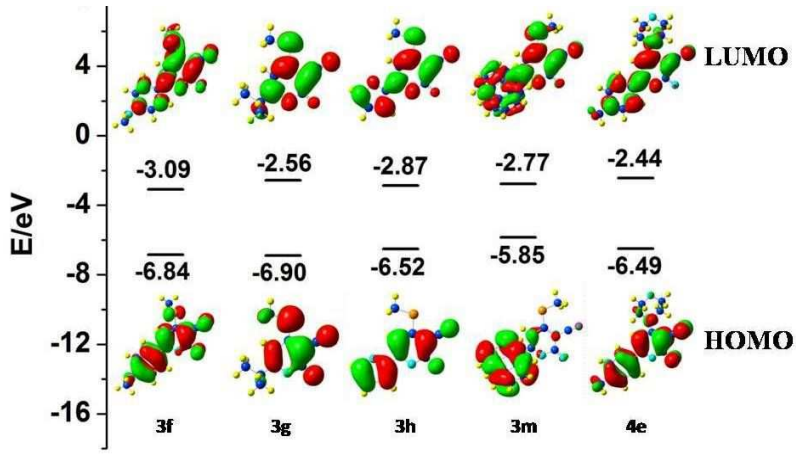

Figure 4. Computed molecular orbital energy diagram and isodensity surface plots of the HOMO, LUMO of dyes **3f**, **3g, 3h, 3m,** and **4e**.

The energies of the HOMO and LUMO levels, HOMO-LUMO gap, main orbital transition, and oscillator strength *f* and ground state dipole moments (μ_g) are listed in Table 2. The

computational results of compounds **3f, 3g, 3h, 3m,** and **4e** revealed that the longer wavelength absorption originates from the HOMO to LUMO electronic excitation (Table 2). The pyranones **3f, 3g, 3h,** and **4e** possessed large dipole moment (10-17 Debye) except **3m** which exhibited low dipole moment (7.24 Debye) possibly due to resultant effect of two dipole vectors in different directions.

Table 2. Computed values of vertical excitations, oscillator strength (*f*), ground state dipole moment (μ_g), assignment, HOMO, LUMO, and energy band gap (E_g) by using B3LYP model.

Entry	λ_{max} (nm)	*f*	μ_g (D)	Assignment	HOMO (eV)	LUMO (eV)	E_g (theo.)
3f	373	0.6651	16.86	HOMO → LUMO (94 %)	-6.84	-3.09	3.75
3g	320	0.2360	13.25	HOMO → LUMO (99%)	-6.90	-2.56	4.34
3h	376	0.6980	10.40	HOMO → LUMO (99 %)	-6.52	-2.87	3.65
3m	489	0.1532	7.24	HOMO → LUMO (97 %)	-5.85	-2.77	3.08
4e	347	0.5378	13.21	HOMO → LUMO (99 %)	-6.49	-2.44	4.05

Electrochemical and Thermal Properties

Electrochemical studies were performed to check the redox behaviour of the compounds **3f**, **3g, 3h, 3m,** and **4e**. Cyclic voltammetric measurements were performed in a three-electrode cell setup using Ag/AgCl as standard electrode and Pt disk as the working electrode, using 2 mM compound and 0.2 M electrolyte tetrabutylammonium hexafluorophosphate (Bu_4NPF_6) dissolved in dry dichloromethane (DCM). All the potentials were calibrated with ferrocene, (Fc/Fc^+). The highest occupied molecular orbital (HOMO) and lowest unoccupied molecular orbital (LUMO) levels were readily estimated from onset oxidation (E_{ox}) and onset reduction

potentials (E_{red}), using the equations $E_{HOMO} = -[(E_{ox} - E_{Fc/Fc^+}) + 4.8]$ eV and $E_{LUMO} = -[(E_{red} - E_{Fc/Fc^+}) + 4.8]$ eV and the data are summarized in Table 3.

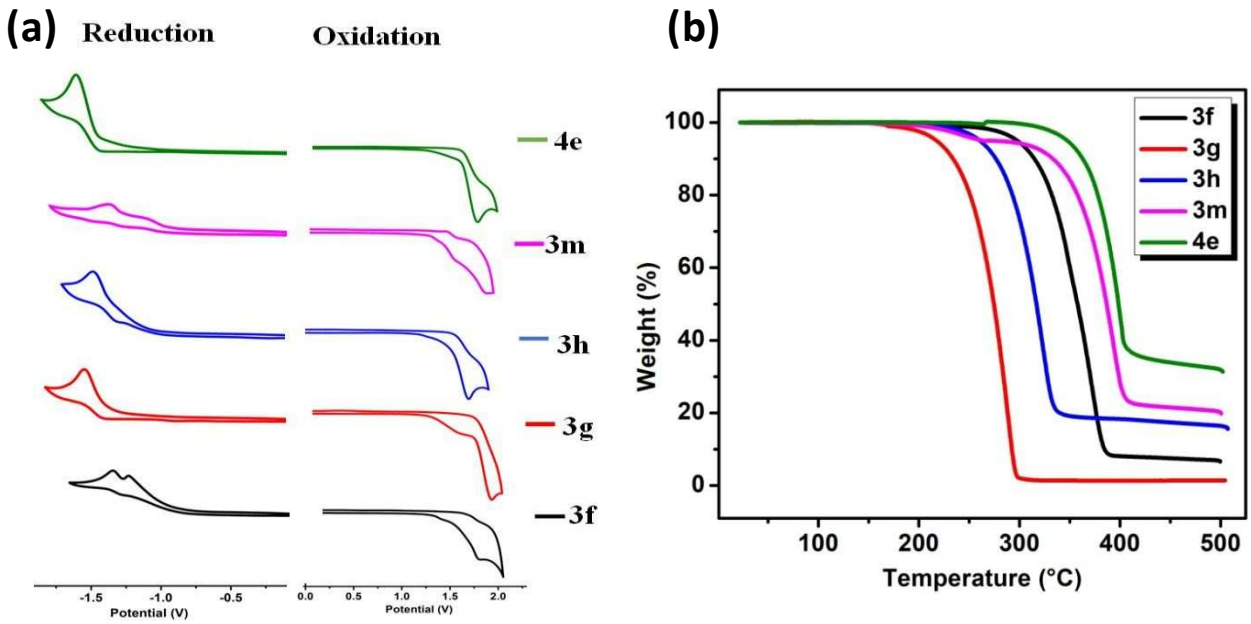

Figure 5. Electrochemical and thermal properties of the dyes **3f, 3g, 3h, 3m** and **4e**: (a) Cyclic voltammogram in dry DCM (scan rate 100 mVs^{-1}) and (b) TGA curves.

Irreversible oxidation and reduction peaks were observed for the dyes **3f**, **3g, 3h, 3m** and **4e** as shown in Figure 5a, which indicated that neither radical cations (oxidized species) nor radical anions (reduced species) are stable entities which may react with solvent molecules or supporting electrolyte. The HOMO values for the compounds **3f, 3g, 3h, 3m,** and **4e** were found to be -6.1, -6.4, -6.1, -5.7, and -6.1 eV respectively whereas LUMO values were in the range of -3.5, -3.0, -3.3, -3.6, and -3.0 eV respectively. The theoretically derived HOMO and LUMO energies and band gaps of the dyes in vacuum were found to be higher than experimentally deduced values from electrochemical measurements in DCM solvent. The deviation in theoretical and experimental values may probably be due to interactions of solvent molecules with the molecules of the dye.

The thermal properties of **3f**, **3g, 3h, 3m,** and **4e** were gauged by thermo gravimetric analysis (TGA) and differential scanning calorimetry (DSC) experiments under argon atmosphere. The melting temperature obtained by DSC experiments for the dyes **3f**, **3g, 3h, 3m,** and **4e** was 225, 168, 218, 267, and 267 ˚C respectively (Supplementary Information Figure S1-S5). All the dyes showed good thermal stability with its 5% weight loss temperatures under argon atmosphere were found to be 298, 218, 260, 263, and 347 ˚C respectively as shown in Table 3.

Table 3. Thermal and electrochemical properties of dyes **3f, 3g, 3h, 3m** and **4e**.

Entry	T_m[a] (˚C)	T_d[b] (˚C)	HOMO (eV)	LUMO (eV)	E_{o-o}[c] (eV)
3f	225	298	-6.1	-3.5	2.6
3g	168	218	-6.4	-3.0	3.4
3h	218	260	-6.1	-3.3	2.8
3m	267	263	-5.7	-3.6	2.1
4e	267	347	-6.1	-3.0	3.1

[a]Melting temperature gauged by DSC. [b]Decomposition temperature (5% weight loss) under nitrogen atmosphere in the TGA measurements. [c]Optical band gap from CV.

On the basis of interesting photophysical, thermal, and electrochemical properties, the dyes **3f**, **3g, 3h, 3m** and **4e** were used to demonstrate their potential application in OLEDs.

OLED DEVICE FABRICATION AND MEASUREMENTS

Materials

Indium tin oxide (ITO) coated glass substrates with a sheet resistance of 15 Ω/sq and light transmittance greater than 88% was purchased from the Luminescence Technology Co., Taiwan. The hole injection material poly(3,4-ethylenedioxythiophene)-poly(styrenesulfonate) (PEDOT:PSS)

with a purity of 99.9% was purchased from UniRegion Bio-Tech Co., Taiwan. The sublimated grade 4,4′-bis(9-carbazolyl)-1,1′-biphenyl,4,4-N,N′-dicarbazole-1,1′-biphenyl (CBP) as host and 2,2′,2"-(1,3,5-benzinetriyl)-tris(-phenyl-1H-benzimidazole) (TPBi) as electron transporting and hole blocking material was purchased from Wang Shine Co., Taiwan. Lithium fluoride (LiF) (purity 99.95%) was purchased from Sigma-Aldrich. Aluminum (Al) ingots (99.999%) were purchased from Showa Chemical Co. Ltd., Taiwan. All materials were used without further purification.

Electroluminescence properties

The solution-processed OLED devices were fabricated with a structure of ITO (125 nm)/ PEDOT:PSS (35 nm)/ CBP:dye (25 nm)/ TPBi (40 nm)/ LiF (1 nm)/ Al (100 nm). The pre-patterned indium tin oxide glass substrates were cleaned with routine procedure, acetone and ethanol by ultrasonic bath for 30 min in each step. Afterward, the substrates were dried with nitrogen (N_2) gas flow and then loaded into a UV-ozone chamber for 15 min to eliminate all organic impurities. PEDOT:PSS was spin-coated (4000 rpm, 20 s) as a hole injection layer on ITO glass in an ambient condition and was annealed at 120 °C for 15 min in an inert atmosphere. Before depositing the following emissive layers, the solution was prepared by dissolving the CBP host and pyranone dyes (**3m**, **3f**, **3h**, **3g,** and **4e**) separately in THF with continuous stirring at 40 ^{o}C for 60-75 min. Then, both the solutions were mixed together to obtain different blending ratios (0.5, 1, 3, and 5 wt%). The resulting solution was then spin-coated at 2500 rpm for 20 s inside the N_2 filled glove box. The depositions of the electron transporting layer (TPBi), electron injection layer (LiF), and the top electrode (Al) were thermally evaporated in sequence over the emissive layer in an ultra-high vacuum chamber at a base pressure of less than 6×10^{-6} torr. All the devices were measured immediately after fabrication in ambient atmospheric condition without further encapsulation.

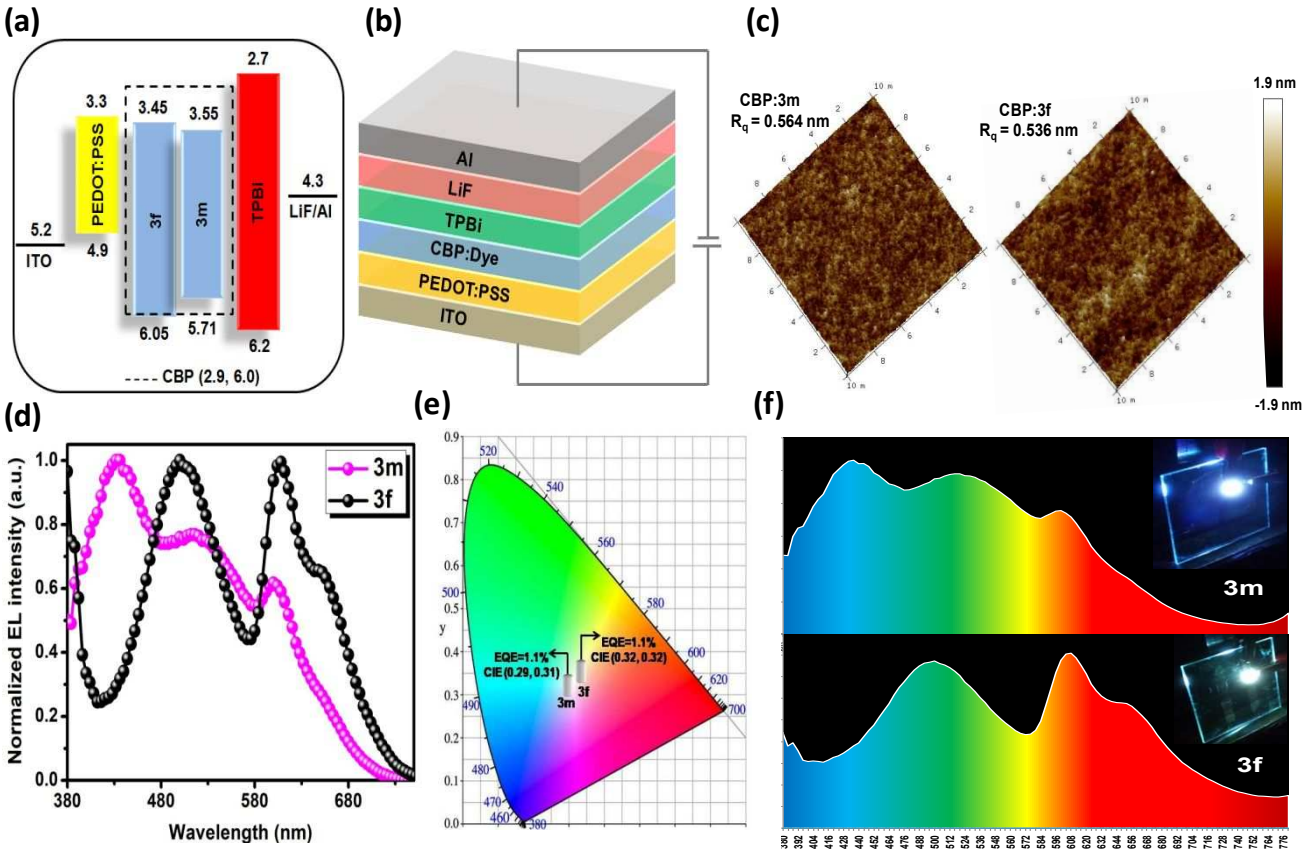

Figure 6. Device fabrication and EL measurements; (a) energy level diagram of the solution processed OLED devices composing pyranones **3f** and **3m** emitters with molecular host CBP; (b) schematic illustration of the device configuration; (c) AFM 3D topographical images of **3m** and **3f**; (d) resultant electroluminescence spectra (1 wt%) of the devices; (e) CIE chromaticity diagram of the devices; (f) electroluminance spectra with chromaticity and device photograph (Inset).

Electroluminescence spectra, luminance, and CIE chromatic coordinate information of the resulting OLEDs were measured by a Photo Research SpectraScan PR655 photometer. A Keithley 2400 electrometer was used to measure the current-voltage (I-V) characteristics. The EL spectra and CIE coordinate, as well as luminance were recorded at each measurement step. The emission area of the devices was 0.25 cm^2, and only the luminance in the forward direction was measured. Since the good film-forming characteristics of light emitting dyes are crucial for the total performance of the devices, atomic force microscopy (AFM) was used to quantitatively investigate the surface morphology of the spin coated new compounds, **3f, 3g, 3h, 3m,** and **4e** on the glass substrate in the tapping mode. Figure 6 illustrated the device configuration, surface morphology, and

electroluminescent properties of the fabricated OLEDs containing the newly synthesized emitters, **3f** and **3m** (1 wt%) with CBP host (For device configuration and surface morphology of **3h, 3g,** and **4e**, see Figure S6 in Supporting Information). For a direct comparison, we prepared thin films of the emissive layers (1 wt% emitter) doped in CBP host under inert atmosphere. The scanning area for each film was 10×10 (μm×μm). Interestingly, all the spin coated layers were found to be smooth as shown in Figure 6c (Figure S6b in Supporting Information) and no apparent cracks or pinholes were observed. The root mean square surface roughness (Rq) values of the dyes **3f, 3g, 3h, 3m,** and **4e** were 0.54 nm, 0.54 nm, 0.70 nm, 0.56 nm, and 0.55 nm, respectively. Each film displayed sufficiently low Rq, which confirmed that all the films have good integrity and stability. In addition, the resulting electroluminescence spectra of the devices **3f** and **3m** exhibited broad band covering the entire visible region from 400 to 700 nm, leading to white light as depicted in Figure 6.

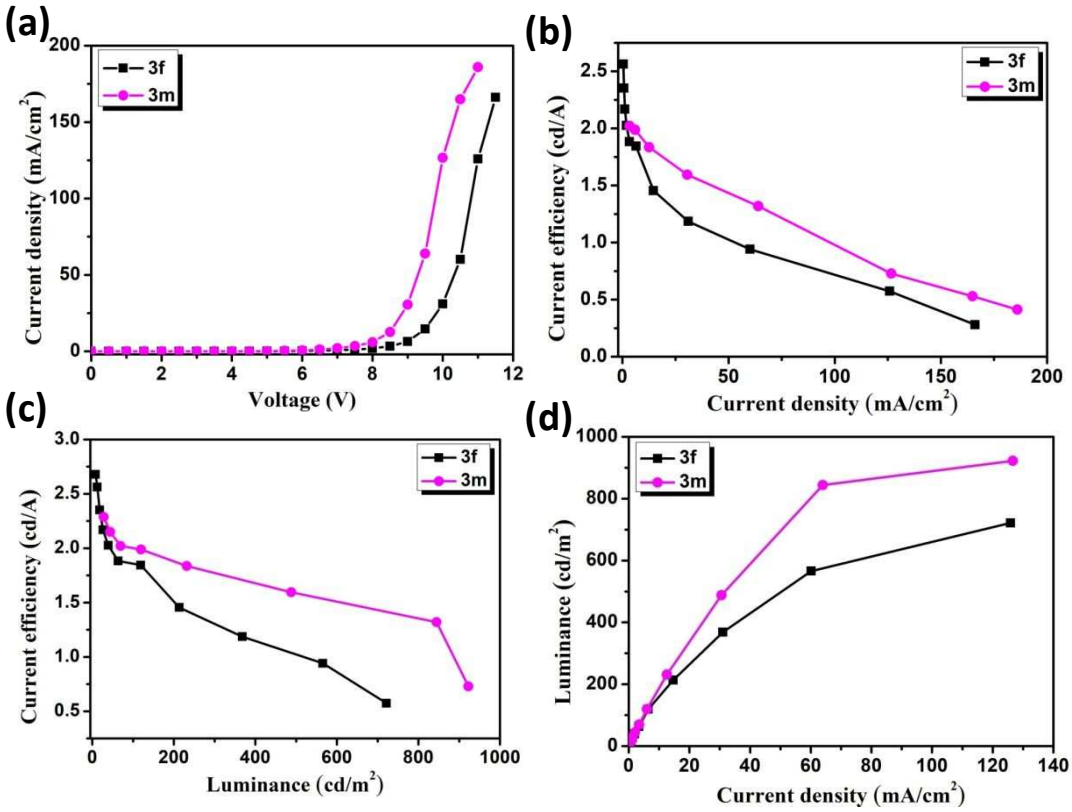

Figure 7. (a) Current density-voltage, (b) current efficiency-current density, (c) current efficiency-luminance, and (d) luminance-current density plots of the solution processed OLED devices composed of 1 wt% **3f** and **3m** emitters.

Figure 7 and Table 4 showed the electroluminescence characteristics of CBP host based solution-processed OLED devices of pyranones **3m** and **3f**. The doping concentration of the emitters strongly influenced the device performance and light-behaviour. The device fabricated with the emitter **3m** (0.5 wt%) doped in CBP host showed relatively best performance with an external quantum efficiency (EQE), power efficiency (PE), and current efficiency (CE) as 1.9%, 1.3 lmW^{-1}, and 2.6 cdA^{-1} at 100 cdm^{-2}, respectively. Interestingly, it showed low turn-on voltage compared to other device fabricated with the emitters **3f, 3g, 3h,** and **4e**. As the concentration increased to 1 wt%, device **3m** exhibited an EQE of 1.1%, current efficiency of 2.0 cdA^{-1}, power efficiency of 0.8 lmW^{-1}, and CIE coordinates of (0.29, 0.31). Furthermore, a significant decrement into the EQE of OLED devices was observed with increasing concentration of dopant (3-5 wt%). For examples, as the concentration of molecule **3m** increased from 1 wt% to 5 wt%, the EQE of device dropped from 1.1% to 0.2% (a 5.5 fold decrement). The good performance of the device at low doping ratios may be attributed to the dilution effect, which may arise from the uniform dispersion of dye in the employed host.[43] At high doping ratio, the poor performance of the device **3m** may be due to charge-carrier imbalance,[43-51] crystallinity of compounds,[43-51] or non-radiative excited state decay due to Auger recombination.[52] The device **3m** exhibited pure white light emission with a maximum brightness 922 cdm^{-2} at 1 wt% and CIE coordinates of (0.29, 0.31), which is possibly attributed to the balanced effect of holes and electrons within the emitting layer. The device formed by using 0.5 wt% **3f** emitter showed pure white light spectrum with a current efficiency of 1.9 cdA^{-1}, EQE of 1.2%, power efficiency of 0.8 lmW^{-1}, and CIE coordinates of (0.32, 0.32) at 100 cdm^{-2}. The WOLED **3f** also exhibited a maximum brightness of 722 cdm^{-2} at 1 wt% with CIE coordinate (0.35, 0.36). The doped devices exhibited better efficiency and luminance when compared to non-doped

(neat film) devices of analogous dyes. It might be due to the effective capturing of excitons formed in CBP host by dopants through favorable energy transfer.

Table 4. Effects of doping concentrations on the operation voltage (OV), power efficiency (PE), current efficiency (CE), external quantum efficiency (EQE), CIE coordinates, and maximum luminance of the solution processed OLED devices.

Emitter	Dopant (wt%)	OV (V)	PE (lmW^{-1})	CE (cdA^{-1}) @100 cdm^{-2}	EQE (%)	CIE coordinates	Maximum luminance (cdm^{-2})
3m	**0.5**	**6.5**	**1.3**	**2.6**	**1.9**	**(0.27, 0.23)**	**836**
	1	**7.8**	**0.8**	**2.0**	**1.1**	**(0.29, 0.31)**	**922**
	3	11.1	0.4	1.4	0.6	(0.33, 0.43)	782
	5	8.7	0.2	0.5	0.2	(0.34, 0.49)	708
	Neat film	-	-	-	-	-	-
3f	**0.5**	**7.1**	**0.8**	**1.9**	**1.2**	**(0.32, 0.32)**	**592**
	1	**8.8**	**0.7**	**1.9**	**1.1**	**(0.35, 0.36)**	**722**
	3	10.6	0.3	1.2	0.6	(0.35, 0.41)	635
	5	9.1	0.2	0.6	0.3	(0.28, 0.35)	544
	Neat film	-	-	-	-	-	-

The **3g** emitter containing device showed a current efficiency of 0.4 cdA^{-1}, EQE of 0.8%, power efficiency of 0.2 lmW^{-1}, and CIE coordinates (0.18, 0.13) (Supplementary Information Table S2 and Figure S7). Whilst, the 0.5 wt% **3h** containing device showed a current efficiency of 0.3 cdA^{-1}, EQE of 0.3%, power efficiency of 0.1 lmW^{-1}, and CIE coordinates (0.21, 0.21). Furthermore, the device with 0.5 wt% **4e** showed a current efficiency, EQE and power efficiency of 0.4 cd A^{-1}, 0.8% and 0.2 lmW^{-1} respectively with CIE coordinate of (0.18, 0.14). The devices **3g, 3h,** and **4e** showed maximum brightness at 1 wt% composition (Figure S7).

It is interesting to note that the electroluminescence spectra of the synthesized dyes **3f, 3g, 3h, 3m** and **4e** exceedingly depend on the substituents present on the pyranone scaffold. In case of device prepared using pyranones **3f** and **3m** containing 4-methoxyphenyl and anthracenyl moiety at position 6, the EL spectra showed broad emission covering entire visible region which was in close agreement with PL spectra of aggregates of the dyes as shown in Figure 2 and Figure 6d. In addition, the EL spectra of devices **3g, 3h,** and **4e** showed close resemblance with the PL spectra of the respective dyes in solid state (Figure 1 and Figure S8) indicating that the EL originated from the radiative decay of singlet excitons localized on the guest and no aggregation present between the molecules in the film.

CONCLUSION

In conclusion, we have synthesized a series of pyranone dyes substituted with donor - acceptor functionalities and demonstrated their photophysical, thermal, electrochemical, and optoelectronic properties. Photophysical analysis of these dyes revealed that five compounds **3f**, **3g, 3h, 3m,** and **4e** showed highly bright fluorescence in the solid state. Among them, dyes **3f** and **3m** showed aggregation-induced emission behaviour in THF/water mixture (0-99%) covering entire visible region. The computational studies using Gaussian software showed that the longer wavelength transitions of **3f, 3g, 3h, 3m,** and **4e** occur from HOMO to LUMO, which involve the charge transfer from the donor segment to the nitrile acceptor group. The cyclic voltammetry analysis of all the dyes revealed irreversible oxidation and reduction process. The OLEDs of **3f**, **3g, 3h, 3m,** and **4e** were successfully fabricated, which exhibited good electroluminescence properties with low turn-on voltage and achieved maximum brightness of 722, 590, 370, 922, and 441 cdm^{-2}, respectively. Among all the five devices (**3f**, **3g, 3h, 3m,** and **4e**), two devices fabricated using the dyes **3f** (4-methoxyphenyl-pyranone at 0.5 and 1 wt%) and **3m** (6-anthracenyl-pyranone at 1 wt%) exhibited pure white light emission with good external

quantum efficiency and brightness. These primary results indicated that the fluorescent donor-acceptor pyranones have promising applications for future OLED display and solid-state lighting.

EXPERIMENTAL SECTION

***General**:* ^{1}H and ^{13}C NMR spectra were recorded at 300 and 400 MHz in Bruker spectrometer. $CDCl_3$ and DMSO-d_6 were taken as solvents. Chemical shifts are reported in parts per million shift (δ-value) from Me_4Si (δ 0 ppm for ^{1}H) or based on the middle peak of the solvent ($CDCl_3$) (δ 77.00 ppm for ^{13}C NMR) as an internal standard. Signal pattern are indicated as s, singlet; d, doublet; dd, double doublet; t, triplet; m, multiplet. Coupling constant (*J*) are given in hertz. Infrared (IR) spectra were recorded in KBr disc and reported in wave number (cm^{-1}). ESIMS spectrometer was used for mass spectra analysis. High resolution mass spectra were taken with a Q-TOF analyzer. The cyclic voltammograms were obtained by CV analyzer and was employed to evaluate highest occupied molecular orbital (HOMO) and lowest unoccupied molecular orbital (LUMO) energy level. All the reactions were monitored by TLC and visualization was done by UV-light (354 nm).

General procedure for the synthesis of 3a-3m** and **4a-4h: A mixture of methyl 2-cyano-3,3-dimethylsulfanylacrylate **1** (2.03 g, 10 mmol), substituted acetophenones **2** (11 mmol) and powdered KOH (15 mmol) in DMSO (50 mL) was stirred at room temperature for 10-14h. After completion, the reaction mixture was poured into ice water with constant stirring. The precipitate thus obtained was filtered and purified on a silica gel column using chloroform as eluent to yield 6-aryl-2-oxo-4-methylsulfanyl-2*H*-pyran-3-carbonitriles **3a-3m**. The compound **3c** (277 mg, 1 mmol), **3d** (320 mg, 1mmol) **3e** (257 mg, 1mmol) was refluxed in methanol with piperidine (127 µl, 1.5 mmol) for 6-7 h, the reaction mixture was cooled to room temperature and the solid obtained was filtered and washed with methanol to furnish **4a**, **4c**, **4f** in good yields and the same procedure was followed with pyrrolidine and morpholine to obtain **4b**, **4d**, **4h**, **4e** and **4g** in good to moderate yield .The 2*H*-

pyran-2-ones **3a-m** and **4a-h** were synthesized according to the procedure described earlier.[41] The data of all the synthesized compounds are given here.

4-(methylthio)-6-(4-nitrophenyl)-2-oxo-2*H*-pyran-3-carbonitrile (3a). Pale Yellow solid (1.42 g, 45% yield); R_f = 0.35 (chloroform/methanol, 99:1, v/v); mp (chloroform/methanol) 244-246 °C; MS (ESI) m/z 289 $[M + H]^+$; IR (KBr) ν = 2214 (CN), 1716 (CO) cm^{-1}; ^1H NMR (400 MHz, DMSO-d_6): δ = 2.87 (s, 3H), 7.41 (s, 1H), 8.29 (d, J = 9.06 Hz, 2H), 8.39 (d, J = 9.06 Hz, 2H) ppm; $^{13}C\{^1H\}$ NMR (100 MHz, DMSO-d_6): δ = 14.9, 91.3, 102.4, 114.4, 124.6, 128.8, 136.0, 149.8, 157.2, 158.7, 171.9 ppm; HRMS (ESI) calculated for $C_{13}H_8N_2O_4S$: 289.0283 $[M + H]^+$. Found 289.0284.

6-(4-fluorophenyl)-4-(methylthio)-2-oxo-2*H*-pyran-3-carbonitrile (3b). Greenish yellow (2 g, 70% yield); R_f = 0.43 (chloroform/methanol, 99:1, v/v); mp (chloroform/methanol) 186-188 °C; MS (ESI) m/z 262 $[M + H]^+$; IR (KBr) ν = 2216 (CN), 1713 (CO) cm^{-1}; ^1H NMR (400 MHz, DMSO-d_6): δ = 2.83 (s, 3H), 7.22 (s, 1H), 7.44 (t, J = 8.8 Hz, 2H), 8.10-8.14 (m, 2H) ppm; $^{13}C\{^1H\}$ NMR (100 MHz, DMSO-d_6): δ = 14.8, 89.4, 99.9, 114.5, 114.5, 116.8, 117.0, 126.8, 130.2, 130.3, 157.5, 160.5, 163.8, 166.3, 172.0 ppm; HRMS (ESI) calculated for $C_{13}H_8FNO_2S$: 262.0338 $[M + H]^+$. Found 262.0333.

6-(4-chlorophenyl)-4-(methylthio)-2-oxo-2*H*-pyran-3-carbonitrile (3c).[41a] Yellow solid (1.8 g, 60% yield); R_f = 0.54 (chloroform/methanol, 99:1, v/v); mp (chloroform/methanol) 240-242 °C; MS (ESI) m/z 278 $[M + H]^+$; IR (KBr) ν = 2217 (CN), 1724 (CO) cm^{-1}; ^1H NMR (400 MHz, DMSO-d_6): δ = 2.83 (s, 3H), 7.25 (s, 1H), 7.66 (d, J = 8.8 Hz, 2H), 8.06 (d, J = 8.8 Hz 2H) ppm; HRMS (ESI) calculated for $C_{13}H_8ClNO_2S$: 278.0043 $[M + H]^+$. Found 278.0039.

6-(4-bromophenyl)-4-(methylthio)-2-oxo-2*H*-pyran-3-carbonitrile (3d).[41a] Yellow solid (1.82 g, 52% yield); R_f = 0.38 (chloroform/methanol, 99:1, v/v); mp (chloroform/methanol)

230-232 °C; MS (ESI) m/z 322 [M + H]$^+$; IR (KBr) ν = 2213 (CN), 1697 (CO) cm^{-1}; ^{1}H NMR (400 MHz, DMSO-d_6): δ = 2.83 (s, 3H), 7.26 (s, 1H), 7.79 (d, J = 8.8 Hz, 2H), 7.98 (d, J = 8.8 Hz 2H) ppm; HRMS (ESI) calculated for $C_{13}H_8BrNO_2S$: 321.9537 [M + H]$^+$. Found 321.9539.

4-(methylthio)-2-oxo-6-(p-tolyl)-2*H*-pyran-3-carbonitrile (3e). Greenish yellow solid (1.83 g, 65% yield); R_f = 0.36 (chloroform/methanol, 99:1, v/v); mp (chloroform/methanol) 220-222 °C; MS (ESI) m/z 258 [M + H]$^+$; IR (KBr) ν = 2212 (CN), 1698 (CO) cm^{-1}; ^{1}H NMR (400 MHz, $CDCl_3$): δ = 2.43 (s, 3H), 2.71 (s, 3H), 6.67 (s, 1H), 7.31 (d, J = 8.12 Hz, 2H), 7.76 (d, J = 8.32 Hz 2H) ppm; ^{13}C{^{1}H} NMR (100 MHz, $CDCl_3$): δ = 14.8, 21.6, 90.4, 97.3, 113.4, 126.7, 127.0, 130.1, 144.0, 157.4, 162.3, 169.8 ppm; HRMS (ESI) calculated for $C_{14}H_{11}NO_2S$: 258.0589 [M + H]$^+$. Found 258.0585.

6-(4-Methoxyphenyl)-4-(methylthio)-2-oxo-2*H*-pyran-3-carbonitrile (3f).[41a] Yellow-Green solid (2.70 g, 90% yield); R_f = 0.28 (chloroform/methanol, 99:1, v/v); mp (chloroform/methanol) 227-228 °C; MS (ESI) m/z 274 [M + H]$^+$; IR (KBr) ν = 2206 (CN), 1711 (CO) cm^{-1}; ^{1}H NMR (400 MHz, $CDCl_3$): δ = 2.69 (s, 3H), 3.89 (s, 3H), 6.60 (s, 1H), 6.99 (d, J = 8.96 Hz, 2H), 7.83 (d, J = 8.92 Hz, 2H) ppm; HRMS (ESI) calculated for $C_{14}H_{12}NO_3S$: 274.0538 [M + H]$^+$. Found 274.0535

6-Isopropyl-4-(methylthio)-2-oxo-2*H*-pyran-3-carbonitrile (3g). White solid (1.88 g, 82% yield); R_f = 0.52 (chloroform/methanol, 99:1, v/v); mp 170-171 °C; MS (ESI) m/z 210 [M + H]$^+$; IR (KBr) ν = 2225 (CN), 1729 (CO) cm^{-1}; ^{1}H NMR (400 MHz, $CDCl_3$): δ = 1.28 (d, J =6.9 Hz, 6H), 2.62 (s, 3H), 2.76-2.83 (m, 1H), 6.09 (s, 1H) ppm; ^{13}C{^{1}H} NMR (100 MHz, $CDCl_3$): δ = 14.6, 19.8, 33.7, 90.8, 98.0, 113.1, 157.7, 170.2, 173.0 ppm; HRMS (ESI) calculated for $C_{10}H_{12}NO_2S$: 210.0589 [M + H]$^+$. Found 210.0587.

6-(furan-2-yl)-4-(methylthio)-2-oxo-2*H*-pyran-3-carbonitrile (3h).[41c] Yellow solid (1.99 g, 78% yield); R_f = 0.65 (chloroform/methanol, 99:1, v/v); mp (chloroform/methanol) 218-219 °C; MS (ESI) m/z 234 $[M + H]^+$; IR (KBr) ν = 2219 (CN), 1732 (CO) cm^{-1}; ^1H NMR (400 MHz, $CDCl_3$): δ = 2.69 (s, 3H), 6.64 (d, J = 1.92, 2H), 7.64 (d, 2H) ppm; HRMS (ESI) calculated for:$C_{11}H_8NO_3S$:234.0225 $[M + H]^+$. Found 234.0223.

4-(methylthio)-2-oxo-6-(thiophen-2-yl)-2*H*-pyran-3-carbonitrile (3i).[41a] Yellow solid (1.36 g, 50% yield); R_f = 0.30 (chloroform/methanol, 99:1, v/v); mp (chloroform/methanol) 253-255 °C; MS (ESI) m/z 250 $[M + H]^+$; IR (KBr) ν = 2205 (CN), 1704 (CO) cm^{-1}; ^1H NMR (400 MHz, DMSO-d_6): δ = 2.79 (s, 3H), 7.13 (s, 1H), 7.33 (dd, J = 3.96 Hz, 5.00 Hz), 8.05 (dd, J = 1.09 Hz, 4.96 Hz, 2H), 8.16 (dd, J = 1.12 Hz, 3.85 Hz, 2H); HRMS (ESI) calculated for $C_{11}H_7NO_2S_2$: 249.9996 $[M + H]^+$. Found 249.9993.

4-(methylthio)-2-oxo-6-(pyridin-2-yl)-2*H*-pyran-3-carbonitrile (3j).[41b] Grey solid (1.2 g, 45% yield); R_f = 0.28 (chloroform/methanol, 98:2, v/v); mp (chloroform/methanol) 205-208°C; MS (ESI) m/z 245 $[M + H]^+$; IR (KBr) ν = 2206 (CN), 1721 (CO) cm^{-1}; ^1H NMR (400 MHz, $CDCl_3$): δ = 2.76 (s, 3H), 7.43-7.46 (m, 1H), 7.56 (s, 1H), 7.88 (td, J = 7.77 Hz, 1.75 Hz, 1H), 8.06-8.09 (m, 1H), 8.68-8.70 (m, 1H); HRMS (ESI) calculated for $C_{12}H_8N_2O_2S$: 245.0385 $[M + H]^+$. Found 245.0383.

4-(methylthio)-2-oxo-6-(pyridin-4-yl)-2*H*-pyran-3-carbonitrile (3k).[41b] Light Grey solid (1.5 g, 56% yield); R_f = 0.22 (chloroform/methanol, 98:2, v/v); mp (chloroform/methanol) 208-210°C; MS (ESI) m/z 245 $[M + H]^+$; IR (KBr) ν = 2214 (CN), 1716 (CO) cm^{-1}; ^1H NMR (400 MHz, $CDCl_3$): δ = 2.76 (s, 3H), 6.83 (s, 1H), 7.68-7.70 (m, 2H), 8.81-8.82 (m, 2H) ppm; HRMS (ESI) calculated for $C_{12}H_8N_2O_2S$: 245.0385 $[M + H]^+$. Found 245.0378.

4-(methylthio)-6-(naphthalen-2-yl)-2-oxo-2*H*-pyran-3-carbonitrile (3l).[41c] Pale yellow solid (2.57 g, 80% yield); R_f = 0.28 (chloroform/methanol, 98:2, v/v); mp

(chloroform/methanol) 248-250 °C; MS (ESI) m/z 294 $[M + H]^+$; IR (KBr) ν = 2213 (CN), 1699 (CO) cm^{-1}; ^1H NMR (400 MHz, DMSO-d_6): δ = 2.87 (s, 3H), 7.35 (s, 1H), 7.61-7.69 (m, 2H), 8.01 (d, J = 7.79 Hz, 1H), 8.07-8.14 (m, 3H), 8.65 (s, 1H) ppm; HRMS (ESI) calculated for $C_{17}H_{11}NO_2S$: 294.0589 $[M + H]^+$. Found 294.0586.

6-(Anthracen-9-yl)-4-(mehtylthio)-2-oxo-2*H*-pyran-3-carbonitrile (3m). Orange solid (2.63 g, 70% yield); R_f = 0.55 (chloroform/methanol, 99:1, v/v); mp (chloroform/methanol) 270-271 ˚C; MS (ESI) m/z 344 $[M + H]^+$; IR (KBr) ν = 2210 (CN) , 1731 (CO) cm^{-1}; ^1H NMR (400 MHz, $CDCl_3$): δ = 2.61 (s, 3H), 6.62 (s, 1H), 7.52-7.59 (m, 4H), 7.88 (d, J = 8.5 MHz 2H), 8.07 (d, J = 8.15 MHz, 2H), 8.64 (s, 1H) ppm; $^{13}C\{^1H\}$ NMR (100 MHz, $CDCl_3$): δ =14.9, 106.1, 113.1, 124.3, 124.5, 125.8, 127.9, 129.0, 130.0, 130.9, 131.1, 157.8, 162.8, 169.6 ppm; HRMS (ESI) calculated for: $C_{21}H_{14}NO_2S$: 344.0745 $[M + H]^+$. Found 344.0746.

6-(4-chlorophenyl)-2-oxo-4-(piperidin-1-yl)-2*H*-pyran-3-carbonitrile (4a). White solid (226 mg, 72% yield); R_f = 0.35 (chloroform/methanol, 98:2, v/v); mp (chloroform/methanol) 223-225˚C; MS (ESI) m/z 315 $[M + H]^+$; IR (KBr) ν = 2210 (CN) , 1680 (CO) cm^{-1}; ^1H NMR (400 MHz, $CDCl_3$): δ = 1.80 (s, 6H), 3.82 (s, 4H), 6.43 (s, 1H), 7.42-7.44 (m, 2H), 7.72-7.74 (m, 2H) ppm; $^{13}C\{^1H\}$ NMR (100 MHz, $CDCl_3$): δ = 23.8, 26.4, 51.0, 72.6, 94.8, 117.2, 125.6, 126.4, 127.5, 129.2, 129.4, 138.2, 159.7, 160.4, 162.2 ppm; HRMS (ESI) calculated for: $C_{17}H_{15}ClN_2O_2$: 315.0900 $[M + H]^+$. Found 315.0901.

6-(4-chlorophenyl)-2-oxo-4-(pyrrolidin-1-yl)-2*H*-pyran-3-carbonitrile (4b).[41c] Off white solid (204 mg, 68% yield); R_f = 0.24 (chloroform/methanol, 98:2, v/v); mp (chloroform/methanol) 308-310 °C; MS (ESI) m/z 301 $[M + H]^+$; IR (KBr) ν = 2201 (CN), 1682 (CO) cm^{-1}; ^1H NMR (400 MHz, DMSO-d_6): δ = 1.94-1.99 (m, 4H), 3.75 (s, 2H), 3.93 (2H), 6.84 (s, 1H), 7.60 (d, J = 8.74 Hz, 2H), 7.96 (d, J = 8.69 Hz, 2H) ppm; HRMS (ESI) calculated for $C_{16}H_{13}ClN_2O_2$: 301.0744 $[M + H]^+$. Found 301.0742.

6-(4-bromophenyl)-2-oxo-4-(piperidin-1-yl)-2*H*-pyran-3-carbonitrile (4c).[41a] Off white (287 mg, 80% yield); R_f= 0.26 (chloroform/methanol, 98:2, v/v); mp (chloroform/methanol) 250-252 °C; MS (ESI) m/z 359 $[M + H]^+$; IR (KBr) ν = 2210 (CN), 1679 (CO) cm^{-1}, ^1H NMR (400 MHz, DMSO-d_6): δ = 1.68 (s, 6H), 3.86 (s, 4H), 7.08 (s, 1H), 7.72-7.75 (m, 2H), 7.89-7.92 (m, 2H) ppm; HRMS (ESI) calculated for $C_{17}H_{15}BrN_2O_2$: 359.0395 $[M + H]^+$. Found 359.0392.

6-(4-bromophenyl)-2-oxo-4-(pyrrolidin-1-yl)-2*H*-pyran-3-carbonitrile (4d).[41c] Off white solid (269 mg, 78% yield); R_f = 0.28 (chloroform/methanol, 98:2, v/v); mp (chloroform/methanol) 306-308 °C; MS (ESI) m/z 345 $[M + H]^+$; IR (KBr) ν = 2204 (CN), 1680 (CO) cm^{-1}; ^1H NMR (400 MHz, DMSO-d_6): δ = 1.93-1.98 (m, 4H), 3.74 (s, 2H), 3.92 (s, 2H), 6.84 (s, 1H), 7.72-7.75 (m, 2H), 7.87-7.89 (m, 2H) ppm; HRMS (ESI) calculated for $C_{16}H_{13}BrN_2O_2$: 345.0239 $[M + H]^+$. Found 345.0234.

4-Morpholino-2-oxo-6-(*p*-tolyl)-2*H*-pyran-3-carbonitrile (4e). Green solid (222 mg, 75% yield); R_f = 0.55 (chloroform/methanol, 98:2, v/v); mp (chloroform/methanol) 264-265 ˚C; MS (ESI) m/z 297 $[M + H]^+$; IR (KBr) ν = 2212 (CN), 1705 (CO) cm^{-1}; ^1H NMR (400 MHz, DMSO-d_6): δ = 2.38 (s, 3H), 3.75 (t, 4H), 3.92 (t, 4H), 7.05 (s, 1H), 7.35 (d, J = 8.0 Hz, 2H), 7.88 (d, J = 8.3MHz, 2H) ppm; $^{13}C\{^1H\}$ NMR (100 MHz, DMSO-d_6): δ = 21.5, 49.9, 66.5, 71.0, 95.3, 118.1, 126.7, 128.2, 130.1, 142.6, 160.0, 161.2, 162.3 ppm; HRMS (ESI) calculated for $C_{17}H_{17}N_2O_3$: 297.1239 $[M + H]^+$. Found 297.1236.

2-oxo-4-(piperidin-1-yl)-6-(p-tolyl)-2*H*-pyran-3-carbonitrile (4f). Brown solid (205 mg, 70% yield); R_f= 0.35 (chloroform/methanol, 98:2, v/v); mp (chloroform/methanol) 194-196 °C; MS (ESI) m/z 295 $[M + H]^+$; IR (KBr) ν = 2191 (CN), 1695 (CO) cm^{-1}; ^1H NMR (400 MHz, $CDCl_3$): δ = 1.79 (s, 6H), 2.40 (s, 3H), 3.81 (s, 4H), 6.41 (s, 1H), 7.25-7.27 (m, 2H), 7.69 (d, J = 8.35 Hz, 2H) ppm; $^{13}C\{^1H\}$ NMR (100 MHz, $CDCl_3$): δ = 21.5, 23.8, 26.3,

50.8, 72.1, 93.8, 117.4, 126.1, 127.9, 129.7, 142.6, 160.7, 161.0, 162.6 ppm; HRMS (ESI) calculated for $C_{18}H_{18}N_2O_2$: 295.1447 $[M + H]^+$. Found 295.1449.

4-morpholino-2-oxo-6-(thiophen-2-yl)-2*H*-pyran-3-carbonitrile (4g).[41c] Greenish Yellow solid (193 mg, 67% yield); R_f = 0.32 (chloroform/methanol, 98:2, v/v); mp (chloroform/methanol) 253-255 °C; MS (ESI) m/z 289 $[M + H]^+$; IR (KBr) ν = 2206 (CN), 1694 (CO) cm^{-1}; ^1H NMR (400 MHz, DMSO-d_6): δ = 3.74-3.76 (m, 4H), 3.90 (t, J = 4.8 Hz 4H), 7.02 (s, 1H), 7.27-7.29 (m, 1H), 7.93 (dd, J = 1.2 Hz,4.8 Hz 1H), 8.02 (dd, J = 1.2 Hz,4.00 Hz 1H) ppm; HRMS (ESI) calculated for $C_{14}H_{12}N_2O_3S$: 289.0647 $[M + H]^+$. Found 289.0647.

6-(naphthalen-2-yl)-2-oxo-4-(pyrrolidin-1-yl)-2*H*-pyran-3-carbonitrile (4h).[41d] White solid (234 mg, 74% yield); R_f = 0.35 (chloroform/methanol, 98:2, v/v); mp (chloroform/methanol) 300-302 ˚C; MS (ESI) m/z 317 $[M + H]^+$; IR (KBr) ν = 2201 (CN), 1686 (CO) cm^{-1}; ^1H NMR (400 MHz, DMSO-d_6): δ = 2.02 (s, 4H), 3.91 (s, 4H), 6.93 (s, 1H), 7.60-7.66 (m, 2H), 7.98-8.10 (m, 4H), 8.53 (s, 1H) ppm; HRMS (ESI) calculated for $C_{20}H_{16}N_2O_2$: 317.1290 $[M + H]^+$. Found 317.1262.

ASSOCIATED CONTENT

Supporting Information: The Supporting Information is available free of charge on the ACS Publications website at DOI:

Thermogravimetric (DSC) analysis of compound **3f, 3g, 3h, 3m,** and **4e;** Electroluminescent properties of OLED devices fabricated with dyes **3g, 3h** and **4e;** Coordinates and absolute energies of compounds **3f, 3g, 3h, 3m,** and **4e;** Copies of ^1H NMR spectra of all the synthesized compounds (**3a-m**, **4a-h**) and ^{13}C NMR spectra of **3a**, **3b**, **3e**, **3g**, **3m**, **4a**, **4e**, **4f**.

AUTHOR INFORMATION

Corresponding Author
*E-mail**:** atul_goel@cdri.res.in
#Equal Authorship

ORCID

Atul Goel: 0000-0003-2758-2461

Jwo-Huei Jou: 0000-0002-9413-0206

Notes

The authors declare no conflict of interest

ACKNOWLEDGMENTS:

AG thanks Department of Atomic Energy (DAE-SRC) India for Outstanding Investigator Award (21/13/2015-BRNS/35029). Authors thank CSIR and UGC, New Delhi for research fellowships. We acknowledge SAIF-CDRI for providing spectral data. The communication number of the manuscript is 9840.

References

(1) Farinola, G. M.; Ragni, R. Electroluminescent materials for white organic light emitting diodes. *Chem. Soc. Rev*. **2011**, *40*, 3467-3482.

(2) Kido, J.; Kimura, M.; Nagai, K. Multilayer white light-emitting organic electroluminescent device. *Science* **1995**, *267*, 1332-1334.

(3) Gong, X.; Wang, S.; Moses, D.; Bazan, G. C.; Heeger, A. J. Multilayer polymer light-emitting diodes: white-light emission with high efficiency. *Adv. Mater.* **2005**, *17*, 2053-2058.

(4) Tonzani, S. Lighting technology: Time to change the bulb. *Nature* **2009,** *459*, 312-314.

(5) Zhang, Z.; Liu, D.; Li, D.; Huang, K.; Zhang, Y.; Shi, Z.; Xie, R.; Han, M.; Wang, Y.; Yang, W. Dual Emissive Cu:InP/ZnS/InP/ZnS Nanocrystals: Single-Source "Greener" Emitters with Flexibly Tunable Emission from Visible to Near-Infrared and Their Application in White Light-Emitting Diodes. *Chem. Mater.* **2015**, *27*, 1405-1411.

(6) Li, X.; Liu, Y.; Song, X.; Wang, H.; Gu, H.; Zeng, H. Intercrossed Carbon Nanorings with Pure Surface States as Low-Cost and Environment-Friendly Phosphors for White-Light-Emitting Diodes. *Angew. Chem.* **2015**, *127*, 1779-1784.

(7) Aharon, E.; Kalina, M.; Frey, G. L. Inhibition of Energy Transfer between Conjugated Polymer Chains in Host/Guest Nanocomposites Generates White Photo- and Electroluminescence. *J. Am. Chem. Soc.* **2006**, *128*, 15968-15969.

(8) Liu, J.; Guo, X.; Bu, L.; Xie, Z.; Cheng, Y.; Geng, Y.; Wang, L.; Jing, X.; Wang, F. White Electroluminescence from a Single-Polymer System with Simultaneous Two-Color Emission: Polyfluorene as Blue Host and 2,1,3-Benzothiadiazole Derivatives as Orange Dopants on the Side Chain. *Adv. Funct. Mater.* **2007**, *17*, 1917-1925.

(9) (a) Wu, Z.; Ma, D.; Recent advances in white organic light-emitting diodes. *Mater. Sci. Eng. R* **2016***, 107,* 1−42. (b) Tsuboi, T. Recent advances in white organic light emitting diodes with a single emissive dopant. *J. Non-Cryst. Solids* **2010**, *356*, 1919–1927. (c) Wu, J.-Y.; Chen, S.-A. Development of a Highly Efficient Hybrid White Organic-Light-Emitting Diode with a Single Emission Layer by Solution Processing. *ACS Appl. Mater. Interfaces* **2018**, *10*, 4851−4859.

(10) Shang, M. M.; Li, C. X.; Lin, J. How to produce white light in a single-phase host? *Chem. Soc. Rev.* **2014**, *43*, 1372-1386.

(11) Green, W. H.; Le, K. P.; Grey, J.; Au, T. T.; Sailor, M. J. White Phosphors from a Silicate-Carboxylate Sol-Gel Precursor That Lack Metal Activator Ions. *Science* **1997**, *276***,** 1826-1828.

(12) Wang, M. S.; Guo, G. C. Inorganic–organic hybrid white light phosphors. *Chem. Commun.* **2016**, *52*, 13194-13204.

(13) Wu, H. B.; Zhou, G. J.; Zou, J. H.; Ho, C. L.; Wong, W. Y.; Yang, W.; Peng, J. B.; Cao, Y. Efficient Polymer White-Light-Emitting Devices for Solid-State Lighting. *Adv. Mater.* **2009**, *21*, 4181-4184.

(14) Luo, J.; Li, X.; Hou, Q.; Peng, Q.; Yang, W.; Cao, Y. High-Efficiency White-Light Emission from a Single Copolymer: Fluorescent Blue, Green, and Red Chromophores on a Conjugated Polymer Backbone. *Adv. Mater.* **2007**, *19*, 1113-11170.

(15) Liang, J.; Zhong, Z.; Li, S.; Jiang, X. F.; Ying, L.; Yang, W.; Peng, J.; Cao, Y. Efficient white polymer light-emitting diodes from single polymer exciplex electroluminescence. *J. Mater. Chem. C* **2017**, *5*, 2397-2403.

(16) Wang, C. L.; Xu, S. H.; Wang, Y. B.; Wang, Z. Y.; Cui, Y. P. Aqueous synthesis of multilayer Mn:ZnSe/Cu:ZnS quantum dots with white light emission. *J. Mater. Chem. C* **2014**, *2*, 660-669.

(17) Singh, N. S.; Sahu, N. K.; Bahadur, D. Multicolor tuning and white light emission from lanthanide doped $YPVO_4$ nanorods: energy transfer studies. *J. Mater. Chem. C* **2014**, *2*, 548-555.

(18) Guo, C.; Huang, D.; Su, Q. Methods to improve the fluorescence intensity of $CaS:Eu^{2+}$ red-emitting phosphor for white LED. *Materials Science and Engineering B* **2006,** *130,* 189-193.

(19) Jang, H. S.; Yang, H.; Kim, S. W.; Han, J. Y.; Lee, S. G.; Jeon, D. Y. White Light-Emitting Diodes with Excellent Color Rendering Based on Organically Capped CdSe Quantum Dots and $Sr_3SiO_5:Ce_3^{3+},Li^+$ Phosphors**.** *Adv. Mater*. **2008**, *20*, 2696-2702.

(20) He, Z.; Zhao, W.; Lam, J. W. Y.; Peng, Q.; Ma, H.; Liang, G.; Shuai, Z.; Tang, B. Z. White light emission from a single organic molecule with dual phosphorescence at room temperature. *Nature Commun.* **2017,** *8*, 416.

(21) Yang, Q. Y.; Lehn, J. M. Bright white-light emission from a single organic compound in the solid state. *Angew. Chem. Int. Ed.* **2014**, *53*, 4572-4577.

(22) Tu, G.; Mei, C.; Zhou, Q.; Cheng, Y.; Geng, Y.; Wang, L.; Ma, D.; Jing, X.; Wang, F. Highly Efficient Pure-White-Light-Emitting Diodes from a Single Polymer: Polyfluorene with Naphthalimide Moieties. *Adv. Funct. Mater* **2006**, *16*, 101-106.

(23) Liu, Y.; Nishiura, M.; Wang, Y.; Zhaomin H. pi-Conjugated Aromatic Enynes as a Single-Emitting Component for White Electroluminescence. *J. Am. Chem. Soc*. **2006**, *128*, 5592-5593.

(24) Zhao, Z.; Xu, B.; Yang, Z.; Wang, H.; Wang, X.; Lu, P.; Tian, W. White Light from Excimer and Electromer in Single-Emitting-Component Electroluminescent Diodes. *J. Phys. Chem. C* **2008**, *112*, 8511–8515.

(25) Pal, K.; Sharma, V.; Koner, A. L. Single-component white-light emission via intramolecular electronic conjugation-truncation with perylenemonoimide. *Chem. Commun.* **2017**, *53*, 7909-7912.

(26) Jin, X. H.; Chen, C.; Ren, C. X.; Cai, L. X.; Zhang, J. Bright white-light emission from a novel donor–acceptor organic molecule in the solid state via intermolecular charge transfer. *Chem. Commun.* **2014**, *50*, 15878-15881.

(27) Zhang, A.; Pan, Q.; Jia, H.; Liu, X.; Xu, B. Synthesis, characteristic and intramolecular energy transfer mechanism of reactive terbium complex in white light emitting diode. *Journal of Rare Earths* **2012**, *30*, 10-16.

(28) Serdiuk, I. E. White Light from a Single Fluorophore: A Strategy Utilizing Excited - State Intramolecular Proton-Transfer Phenomenon and Its Verification. *J. Phys. Chem.C* **2017**, *121*, 5277-5286.

(29) Padalkar, V. S.; Seki, S. Excited-state intramolecular proton-transfer (ESIPT)-inspired solid state emitters. *Chem. Soc. Rev.* **2016**, *45*, 169-202.

(30) Park, S.; Kwon, J. E.; Kim, S. H.; Seo, J.; Chung, K.; Park, S. Y.; Jang, D. J.; Medina, B. M.; Gierschner, J.; Park, S. Y. A White-Light-Emitting Molecule: Frustrated Energy Transfer between Constituent Emitting Centers. *J. Am. Chem. Soc*. **2009**, *131*, 14043-14049.

(31) Fleetham, T.; Huang, L.; Li, J. Tetradentate Platinum Complexes for Efficient and Stable Excimer-Based White OLEDs. *Adv. Funct.Mater.* **2014**, *24*, 6066–6073.

(32) (a) Murphy, L.; Brulatti, P.; Fattori, V.; Cocchi, M.; Williams, J. A. G. Blue-shifting the monomer and excimer phosphorescence of tridentate cyclometallated platinum(II) complexes for optimal white-light OLEDs. *Chem. Commun*. **2012**, *48*, 5817–5819. (b) Llorente, A. G. Excimer emission of Ir complex for solution processed single emitting layer white OLEDs. *Organic Electronics* **2018**, *63*, 305-309.

(33) (a) Wang, H.; Li, Y.; Zhang, Y.; Mei, J.; Su, J. A new strategy for achieving single-molecular white-light emission: using vibration-induced emission (VIE) plus aggregation-induced emission (AIE) mechanisms as a two-pronged approach. *Chem. Commun*. **2019**, *55*, 1879-1882. (b) Zhang, Z.; Tian, R.; Zhou, W.; Lin, Y.; Lu, C. Aggregation-induced emission assembled ultrathin films for white light-emitting diodes. *Chem. Commun.* **2017**, *53*, 12676-12679.

(34) (a) Chen, Z.; Wu, D.; Han, X.; Liang, J.; Yin, J.; Yu, G.A.; Liu, S. H. A novel fluorene-based gold(I) complex with aggregate fluorescence change: a single component white light-emitting luminophor. *Chem. Commun.* **2014**, *50*, 11033-11035. (b) Leng, J.; Li, H.; Chen, P.; Sun, W.; Gao, T.; Yan, P. Aggregation-induced white-light emission from the triple-stranded dinuclear Sm(III) complex. *Dalton Trans*. **2014**, *43*, 12228-12235.

(35) (a) Tu, D.; Leong, P.; Guo, S.; Yan, H.; Lu, C.; Zhao, Q. Highly Emissive Organic Single-Molecule White Emitters by Engineering *o*-Carborane-Based Luminophores. *Angew. Chem.*

Int. Ed. **2017**, *56*, 11370 –11374. (b) Huynh, H. V.; He, X.; Baumgartner, T. Halochromic generation of white light emission using a single dithienophosphole luminophore. *Chem. Commun.* **2013**, *49*, 4899-4901. (c) Liu, W.; Chen, Z.; Zheng, C. J.; Liu, X. K.; Wang, K.; Li, F.; Dong, Y. P.; Ou, X. M.; Zhang, X. H. A novel nicotinonitrile derivative as an excellent multifunctional blue fluorophore for highly efficient hybrid white organic light-emitting devices. *J. Mater. Chem. C* **2015**, *3*, 8817-8823.

(36) Raghuvanshi, A.; Jha, A. K.; Sharma, A.; Umar, S.; Mishra, S.; Kant, R.; Goel, A. A Nonarchetypal 5,6-Dihydro-2*H*-pyrano[3,2-*g*]indolizine-based Solution-Solid Dual Emissive AIEgen with Multicolor Tunability. *Chem. Eur. J.* **2017**, *23* 4527-4531.

(37) Goel, A.; Chaurasia, S.; Dixit, M.; Kumar, V.; Prakash, S.; Jena, B.; Verma, J. K.; Jain, M.; Anand, R. S.; Manoharan, S. S. Donor-Acceptor 9-Uncapped Fluorenes and Fluorenones as Stable Blue Light Emitters. *Org. Lett.* **2009**, *11*, 1289-1292.

(38) (a) Goel, A.; Kumar, V.; Chaurasia, S.; Rawat, M.; Prasad, R.; Anand, R. S. Synthesis, Electrochemical and Optical Properties of Stable Yellow Fluorescent Fluoranthenes. *J. Org. Chem*. **2010**, *75*, 3656-3662. (b) Goel, A.; Kumar, V.; Nag, P.; Bajpai, V.; Kumar, B.; Singh, C.; Prakash, S.; Anand, R. S. Thermally Stable Nonaggregating Pyrenylarenes for Blue Organic Light-Emitting Devices. *J. Org. Chem.* **2011**, *76*, 7474-7481. (c) Goel, A.; Kumar, V.; Singh, S. P.; Sharma, A.; Prakash, S.; Singh, C.; Anand, R. S. Non-aggregating solvatochromic bipolar benzo[f]quinolines and benzo[a] acridines for organic electronics. *J. Mater. Chem.* **2012**, *22*, 14880-14888.

(39) Goel, A.; Ram, V. J. Natural and synthetic 2*H*-pyran-2-ones and their versatility in organic synthesis. *Tetrahedron* **2009**, *65*, 7865-7913.

(40) Singh, F. V.; Parihar, A.; Chaurasia, S.; Singh, A. B.; Singh, S. P.; Tamrakar, A. K.; Srivastava, A. K.; Goel, A. 5, 6-Diarylanthranilo-1,3-dinitriles as a new class of antihyperglycemic agents. *Bioorg. Med. Chem. Lett*. **2009**, *19*, 2158-2161.

(41) (a) Tominaga, Y.; Ushirogouchi, A.; Matsuda, Y.; Kobayashi, G. Synthesis and Reaction of 6-Aryl- and 6-Styryl-3-cyano-4-methylthio-2*H*-pyran-2-ones. *Chem. Pharm. Bull.* **1984**, *32*, 3384-3395. (b) Mizuyama, N.; Kohra, S.; Ueda, K.; Hiraoka, K.; Takahashi, K.; Tominaga, Y. Synthesis and Fluorescence of 4-Methylsulfanyl-6-pyridyl-2*H*-pyran-2-ones in Solid State. *Heterocycles* **2007**, *71*, 399-409. (c) Mizuyama, N.; Murakami, Y.; Kohra, S.; Ueda, K.; Hiraoka, K.; Nagaoka, J.; Takahashi, K.; Shigemitsu, Y.; Tominaga, Y. Synthesis and Fluorescence of 2*H*-Pyrone Derivatives for Organic Light-emitting Diodes (OLED). *J. Heterocyclic Chem*. **2007**, *44*, 115-132. (d) Thimmarayaperumal, S.; Shanmugam, S. Base-Promoted Selective Synthesis of 2*H*-Pyranones and Tetrahydronaphthalenes via Domino Reactions. *ACS Omega* **2017**, *2*, 4900−4910.

(42) Frisch, M. J.; Trucks, G. W.; Schlegel, H. B.; Scuseria, G. E.; Robb, M. A.; Cheeseman, J. R.; Scalmani, G.; Barone, V.; Mennucci, B.; Petersson, G. A.; Nakatsuji, H.; Caricato, M.; Li, X.; Hratchian, H. P.; Izmaylov, A. F.; Bloino, J.; Zheng, G.; Sonnenberg, J. L.; Hada, M.; Ehara, M.; Toyota, K.; Fukuda, R.; Hasegawa, J.; Ishida, M.; Nakajima, T.; Honda, Y.; Kitao, O.; Nakai, H.; Vreven, T.; Montgomery, J. A., Jr.; Peralta, J. E.; Ogliaro, F.; Bearpark, M.; Heyd, J. J.; Brothers, E.; Kudin, K. N; Staroverov, V. N; Kobayashi, R.; Normand, J.; Raghavachari, K.; Rendell, A.; Burant, J. C.; Iyengar, S. S.; Tomasi, J.; Cossi, M.; Rega, N.; Millam, N. J.; Klene, M.; Knox, J. E.; Cross, J. B.; Bakken, V.; Adamo, C.; Jaramillo, J.; Gomperts, R.; Stratmann, R. E.; Yazyev, O.; Austin, A. J.; Cammi, R.; Pomelli, C.; Ochterski, J. W.; Martin, R. L.; Morokuma, K.; Zakrzewski, V. G.; Voth, G. A.; Salvador, P.; Dannenberg, J. J.; Dapprich, S.;

Daniels, A. D.; Farkas, Ö.; Foresman, J. B.; Ortiz, J. V.; Cioslowski, J.; Fox, D. J. Gaussian 09, revision A.02; Gaussian, Inc.: Wallingford, CT, 2009.

(43) De, J.; Gupta, S. P.; Swayamprabha, S. S.; Dubey, D. K.; Bala, I.; Sarkar, I.; Dey, G.; Jou, J. H.; Ghosh, S.; Pal, S. K. Blue Luminescent OLED Devices of a New Class of Star-Shaped Columnar Mesogens Exhibiting π-π Driven Supergelation. *J. Phys. Chem. C* **2018**, *122*, 23659-23674.

(44) Jou, J. H.; Sahoo, S.; Kumar, S.; Yu, H.-H.; Fang, P.-H.; Singh, M.; Krucaite, G.; Volyniuk, D.; Grazuleviciusc, J. V.; Grigalevicius, S. A wet- and dry process feasible carbazole type host for highly efficient phosphorescent OLEDs. *J. Mater. Chem. C* **2015**, *3*, 12297-12307.

(45) Konidena, R. K.; Thomas, K. R. J.; Singh, M.; Jou, J. H. Thienylphenothiazine integrated pyrenes: an account on the influence of substitution patterns on their optical and electroluminescence properties. *J. Mater. Chem. C* **2016**, *4*, 4246-4258.

(46) Bala, I.; Ming, L.; Yadav, R. A. K.; De, J.; Dubey, D. K.; Kumar, S.; Singh, H.; Jou, J. H.; Kailasam, K.; Pal, S. K. Deep-Blue OLED Fabrication from Heptazine Columnar Liquid Crystal Based AIE-Active Sky-Blue Emitter. *ChemistrySelect* **2018**, *3*, 7771-7777.

(47) Joseph, V.; Thomas, K. R. J.; Yang, W. Y.; Yadav, R. A. K.; Dubey, D. K.; Jou, J. H. Tetra-substituted Dipolar Carbazoles: Tuning Optical and Electroluminescence Properties by Linkage Variation. *Asian J. Org. Chem*. **2018**, *7*, 1654-1666.

(48) Pathak, A.; Thomas, K. R. J.; Singh, M.; Jou, J. H. Fine-Tuning of Photophysical and Electroluminescence Properties of Benzothiadiazole-Based Emitters by Methyl Substitution. *J. Org. Chem*. **2017**, *82*, 11512-11523.

(49) Jou, J. H.; Kumar, S.; Fang, P.-H.; Venkateswararao, A.; Thomas, K. R. J.; Shyue, J.-J.; Wang, Y.-C.; Lia, T.-H.; Yua, H.-H. Highly efficient ultra-deep blue organic light emitting diodes

with a wet- and dry-process feasible cyanofluorene acetylene based emitter. *J. Mater. Chem. C* **2015**, *3*, 2182-2194.

(50) Wanga, Y.; Huanga, H.; Wanga, Y.; Zhua, Q.; Qin, J. Simple oxadiazole derivatives as deep blue fluorescent emitter and bipolar host for organic light-emitting diodes. *Optical Materials* **2018**, *84*, 278-283.

(51) Tagarea, J.; Dubey, D. K.; Jou, J. H.; Vaidyanathana, S. Synthesis, photophysical, theoretical and electroluminescence study of triphenylamine-imidazole based blue fluorophores for solution-processed organic light emitting diodes. *Dyes and Pigments* **2019,** *160*, 944-956.

(52) (a) Bae, W. K.; Brovelli, S.; Klimov, V. I. Spectroscopic insights into the performance of quantum dot light-emitting diodes. *MRS Bulletin* **2013**, *38*, 721-730. (b) Hua, S. J.; Lua, Z. H. Ultralow-voltage Auger-electron-stimulated organic light-emitting diodes. *J. Photon. Energy* **2016**, *6*, 036001-12. (c) Bae, W. K.; Park, Y. S.; Jim, J.; Lee, D.; Padilha, P. A.; McDaniel, H.; Robel, I.; Lee, C.; Pietryga1, J. M.; Klimov, V. I. Controlling the influence of Auger recombination on the performance of quantum-dot light-emitting diodes. *Nature Commun.* **2013**, *4*:2661, 1-8.

TOC ABSTRACT